Exciton coupled circular dichroic studies of self-assembled brevetoxin-porphyrin conjugates in lipid bilayers and polar solvents

Stefan Matile, Nina Berova and Koji Nakanishi

Background: Brevetoxins, involved in the 'red tide' as well as shellfish poisoning, are known to bind to cell membranes and membrane proteins. Brevetoxin B (BTX-B) interacts specifically with neuronal sodium channels. We recently found that BTX also induces selective ion movements across lipid bilayers through transmembrane BTX self-assemblies.

Results: We examined the self-assembly of several BTX derivatives in the presence and absence of cations and lipid bilayers using the powerful porphyrin chromophores as circular dichroism labels. BTX derivatives self-assemble into tubes, which can bind to metals both when soluble and when inserted into the bilayer to form transmembrane pores. Depending on the tendency of the BTX derivative to self-aggregate (the critical 'micelle' concentration, cmc), it may aggregate in solution before membrane insertion, or may insert itself into the membrane as a monomer before assembling the pore.

Conclusions: The active BTX-B complex in lipid bilayers is a cyclic, transmembrane self-assembly consisting of antiparallel aligned BTX molecules that can mediate selective ion movement through membranes. The differences in pore formation mechanisms between BTX derivatives may be reflected in differences in pore formation by natural BTX variants, perhaps explaining their varying levels of toxicity.

Address: Department of Chemistry, Columbia University, New York, NY 10027, USA.

Correspondence: Koji Nakanishi
e-mail: kn5@columbia.edu

Key words: brevetoxins, ionophores, pore formation mechanisms, porphyrin reported exciton coupled circular dichroic (CD) method, self-assembly

Received: **18 Mar 1996**
Revisions requested: **5 Apr 1996**
Revisions received: **15 Apr 1996**
Accepted: **2 May 1996**

Chemistry & Biology May 1996, **3**:379–392

Introduction

Polyether marine toxins are attracting increased attention because of human intoxications (shellfish poisoning), massive fish kills (red tide) and the economic and social consequences of such incidents [1–3]. The first structure of a polyether marine toxin to be determined was that of brevetoxin B (BTX-B, compound **1**, Fig. 1) [4,5], and this was also the first of these toxins to be synthesized [6]. The eleven cyclic ethers that make up BTX-B are arranged as a rigid skeleton of trans-fused ether rings interrupted by two hinges that consist of seven- (D, E) and eight- (H) membered rings. We have previously proposed [7] that the factors that are important in the ordered transmembrane arrangement of BTX in lipid bilayers are the rigidity and hydrophobicity of the BTX skeleton, as well as its overall length (~30 Å, which corresponds to the thickness of a lipid bilayer). Most of these features are present in the structures of the large number of brevetoxins and ciguatoxins, which have since been characterized [1–3].

Despite the structural similarities of brevetoxins and ciguatoxins, widely varying biological activities have been reported [1–3]. BTX-B, in particular, has been shown to bind specifically to neuronal sodium channels, resulting in activation, inhibition of inactivation, and stabilization of several of their subconductance states ([8] and references therein). Although BTX-A, an ichthytoxic molecule, exhibits similar effects, BTX-B1 and B3, which have structures closely related to BTX-B, are not ichthyotoxic [2,3]. It is thought that oxidative modifications of BTX-B to derivatives with altered toxicity are part of a self-defense mechanism of the cockles and mussels against toxins originating from the 'red tide' dinoflagellate *Gymnodinium breve*. A molecular-level understanding of the mechanisms of the specific toxic effects of different brevetoxins should be helpful in the rational search for BTX antagonists.

We have recently found that transmembrane BTX-B self-assemblies mediate selective cation movement across lipid bilayers [7]. This observation raises many questions in the fields of both chemistry and biology. Our own main interest focuses on aspects of the structures of supramolecular BTX assemblies in the presence or absence of lipid bilayers and cations, since this should clarify our understanding of BTX bioactivities in lipid bilayers.

Structural studies of non-chromophoric, large supramolecular assemblies in complex systems remain difficult [9,10]. We therefore decided to use the recently developed powerful porphyrin chromophores [11–14] as labels to explore the applicability of the exciton-coupled circular

Figure 1

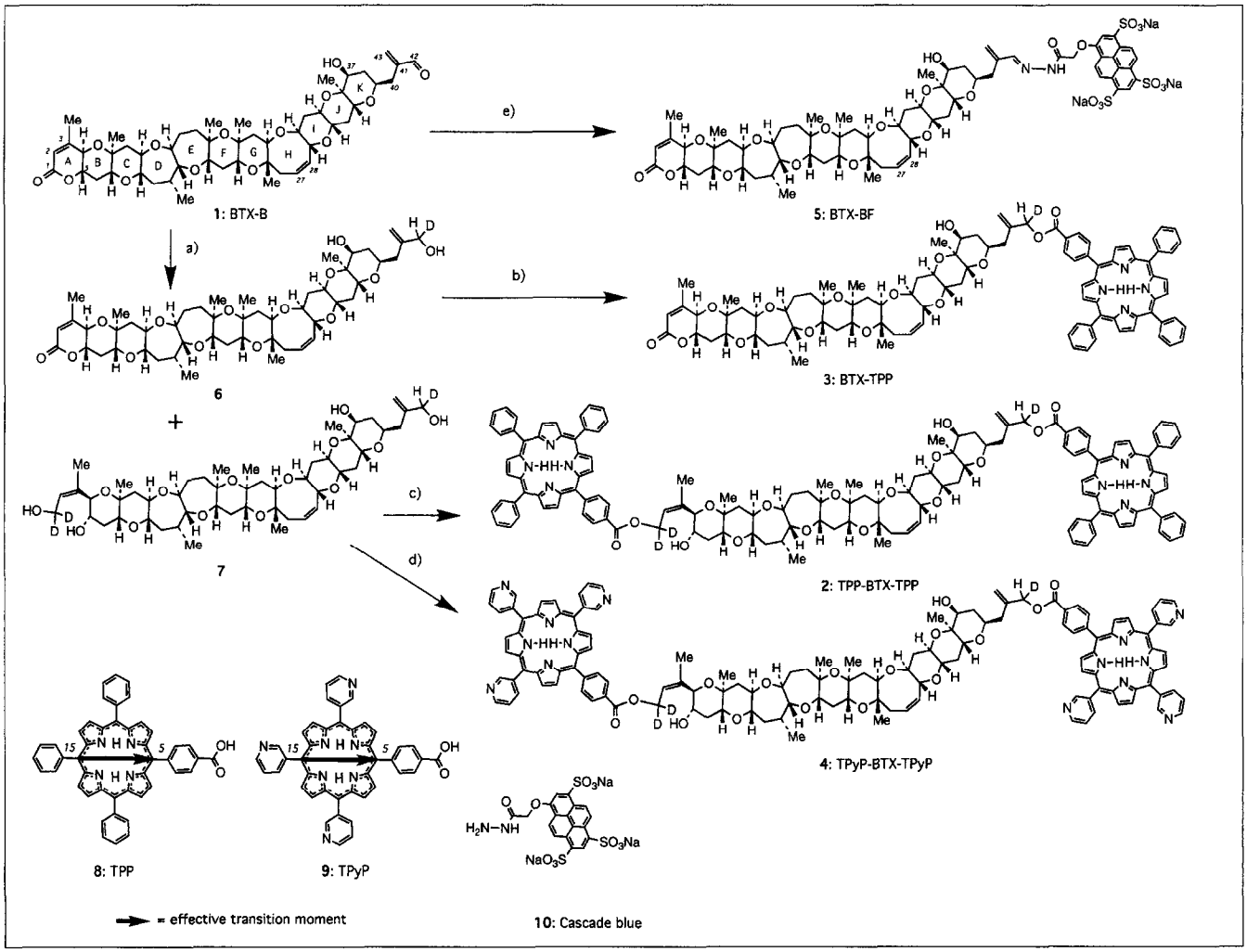

Structure and synthesis of CD- and fluorescence-labeled BTXs. Conditions: **(a)** $NaBD_4$, $CeCl_3$, MeOH, room temperature (RT), 4 min, 41 % (**6**), 37 % (**7**); **(b) 8,** 1-(3-dimethylaminopropyl)-3-ethylcarbodiimide (EDC), dimethyl-4-aminopyridine (DMAP), CH_2Cl_2, RT, 10 h, 92 %; **(c) 8**, EDC, DMAP, RT, 1.5 h, 32 %; **(d) 9**, EDC, DMAP, CH_2Cl_2, RT, 1.5 h, 29 %; **(e) 10**, H_2O, RT, 3 h, quantitative yield.

dichroism (CD) method to structural studies of large molecules in complex systems. This method is a sensitive, non-empirical technique, in which the sign of bisignate Cotton effects between coupled chromophores directly represents their absolute sense of twist, in other words, the absolute configuration and conformation of chiral molecules [15,16]. We have already shown that the superb spectroscopic properties of the porphyrin chromophores, namely the intense and narrow Soret band absorptions around 415 nm, ϵ = 350 000, give rise to coupling between porphyrin residues which are up to 50 Å apart [12]. The exciton-coupled CD amplitudes are sensitive to changes in angle and distance [15]. In the case of long distance couplings, as in brevetoxin bisporphyrin, the bisignate curves are characterized by a non-conservative shape of their weak split Cotton effects, that is, unequal intensities of the two split Cotton effects as opposed to the normal conservative shape [12]. Thus, CD studies of porphyrin-tagged BTX-B molecules **2–4**, in the absence or presence of lipids, should clarify some of the important structural aspects of BTX-B self-assemblies.

Results

CD-labeled BTX-B: brevetoxin–porphyrin conjugates

We prepared several derivatives of BTX-B labeled with *p*-(10,15,20-triphenyl-5-porphyrinyl)benzoic acid/benzoate (TPP), *p*-(10,15,20-tripyrid-3'-yl-5-porphyrinyl)benzoic acid/benzoate (TPyP), or 'cascade blue'. These were: TPP-BTX-TPP, BTX-TPP, TPyP-BTX-TPyP and cascade-blue labeled BTX-B, BTX-BF (compounds **2**, **3**, **4** and **5**, respectively, Fig. 1). Selective reduction of BTX-B (compound **1**) to the diol **6** or tetrol **7** [7,8], was

followed by selective esterification with TPP (compound **8**) or TPyP (compound **9**), respectively, giving the BTX-porphyrin conjugates **2**–**4**. Linkage of the fluorescent cascade blue molecule (compound **10**) to BTX-B (**1**) yielded BTX-BF (**5**) [7].

Self-assembly of BTX-B porphyrin conjugates

The CD spectra of the bisporphyrin BTXs TPP-BTX-TPP (**2**), TPyP-BTX-TPyP (**4**) and monoporphyrin BTX-TPP (**3**) in nonpolar solvents are devoid of distinct Cotton effects above 300 nm. Thus, the porphyrin chromophores are coupled neither intramolecularly nor intermolecularly. This reflects the energy-minimized, monomeric state of all three of these molecules, which share a linear, cigar-shaped conformation of the BTX-B backbone [17], so that the effective transition moments of the pendant chromophores all run in the 5,15 direction (see arrows in compounds **8** and **9**, Fig. 1), in a CD-silent, co-linear alignment [11–14].

Titration of a methanolic solution of hydrophobic TPP-BTX-TPP (**2**) with water gives rise to an intense conservative split CD spectrum (showing similar intensities of positive and negative Cotton effects) with a negative exciton chirality, the intensity becoming maximal around a 1:1 mixture of methanol/water (Fig. 2a); this shows that the TPP-BTX-TPP self-assembly shown as **11** in Figure 2c is formed. The single isochroic point at 418 nm indicates that self-organization of **2** to form **11** is a single-step reaction. The amplitude (A) of the CD spectrum remained unchanged upon dilution of a 2.0 μM solution of **11** in MeOH/water 3:1 down to 0.4 μM, the limit of accurate detectability. Thus, the critical 'micelle' concentration (cmc) of **11** is <0.4 μM.

Similar titration with water of monoporphyrin BTX **3** in methanol yields a different self-assembly (shown as **12** in Fig. 2g). Compared to the bisporphyrin assembly **11** (Fig. 2a), the bisignate CD spectrum of self-assembly **12** (Fig. 2e) comprising monoporphyrin **3** is of opposite sign and weaker (in MeOH/water 1:1, A = –157 for **11** versus A = +59 for **12**). Weak stacking of **3**, which could be due to antiparallel dimers of monoporphyrin **3**, is already present in MeOH (Fig. 2e); self-organization increases with addition of water, and levels off after the proportion of water reaches 50 %. When a 2.8 μM solution in MeOH/water 3:1 solution is further diluted, the CD amplitudes are constant down to 1.7 μM, after which the amplitude decreases significantly, showing that the cmc is at this concentration.

In contrast, the water-soluble hexacation TPyP-BTX-TPyP (**4**), which has six pyridinium moieties, shows a weak non-conservative bisignate couplet in water at pH 4, because the self-organization of **4** to form **13** is inhibited by the charge repulsion of the cationic pyridinium moieties (Fig. 3a). The weak, concentration-independent bisignate CD curve of bisporphyrin **4** in pH 4 water is thus assigned to an intramolecular long distance exciton coupling of monomeric **4** (see below). Similar non-aggregating properties were also observed for the water-soluble trianionic BTX-BF (**5**) at 10 μM, which exhibited only weak CD Cotton effects due to ene-lactone $n\pi^*$ and ene-lactone $\pi\pi^*$ at 254 nm ($\Delta\epsilon$ = +2.7) and 229 nm ($\Delta\epsilon$ = –2.2), respectively, as in the case of BTX-B in MeOH [4].

What are the driving forces leading to the formation of the bis-chromophoric self-assembly **11** and the monochromophoric self-assembly **12** (Fig. 2)? At least four interactions are conceivable: 1) hydrophobic interactions of the BTX backbone; 2) intermolecular hydrogen bridges between two skeletal ether functions mediated by water molecules that act as double hydrogen donors; 3) π,π-stacking of the porphyrin chromophores; and 4) π,π-stacking or hydrophobic attraction of the pendant phenyl substituents. In the three model compounds TPP-BTX-TPP (**2**), BTX-TPP (**3**) and TPyP-BTX-TPyP (**4**), the BTX moieties remain largely unchanged, while the attractive and repulsive forces operating between the porphyrin chromophores vary. As shown in Figure 2a and e, addition of water to methanol solutions of bisporphyrin **2** or monoporphyrin **3** changes the uncharacteristic CD curves into clear bisignate coupled spectra. In contrast, steroids or 3,3'-connected dimeric steroids with porphyrins at both terminals show clear bisignate CD curves due to intramolecular coupling [11,12]; addition of water to methanol solutions transfers these clear bisignate CD curves into nondescript weak signals, caused by inter- and intramolecular porphyrin–porphyrin coupling in disorganized aggregates. The opposite trends observed in the BTX porphyrin conjugates **2** and **3**, in other words, the appearance of coupled CD spectra of opposite signs with increase in medium polarity, thus arises from the water-induced self-organization of BTX backbone moieties, which in turn gives rise to ordered stacking of the porphyrin chromophores, forming the superstructures **11** and **12**.

The porphyrin content in self-assemblies of bischromophoric **11** is double that of the monochromophoric assembly **12** (Fig. 2), which has a larger cmc and a CD of smaller amplitude and opposite sign. It should be noted that the bisignate CD curves of **11** and **12** are a result of chiral stacking of porphyrin chromophores induced by the self-assembly of chiral BTX molecules. The opposite signs in the split CDs, negative for **11** and positive for **12**, show that the dihedral angles between the coupling transition moments, that is, the 5,15 axis of the porphyrins [11,12], are negative and positive, respectively, in **11** and **12**. In aqueous polar media, the BTX backbones in assemblies **11** and **12** must be organized by the ether oxygens, which are hydrogen-bonded to water molecules, and by the hydrophobic interactions between the BTX skeletons. All ether oxygens outside and inside the BTX

Figure 2

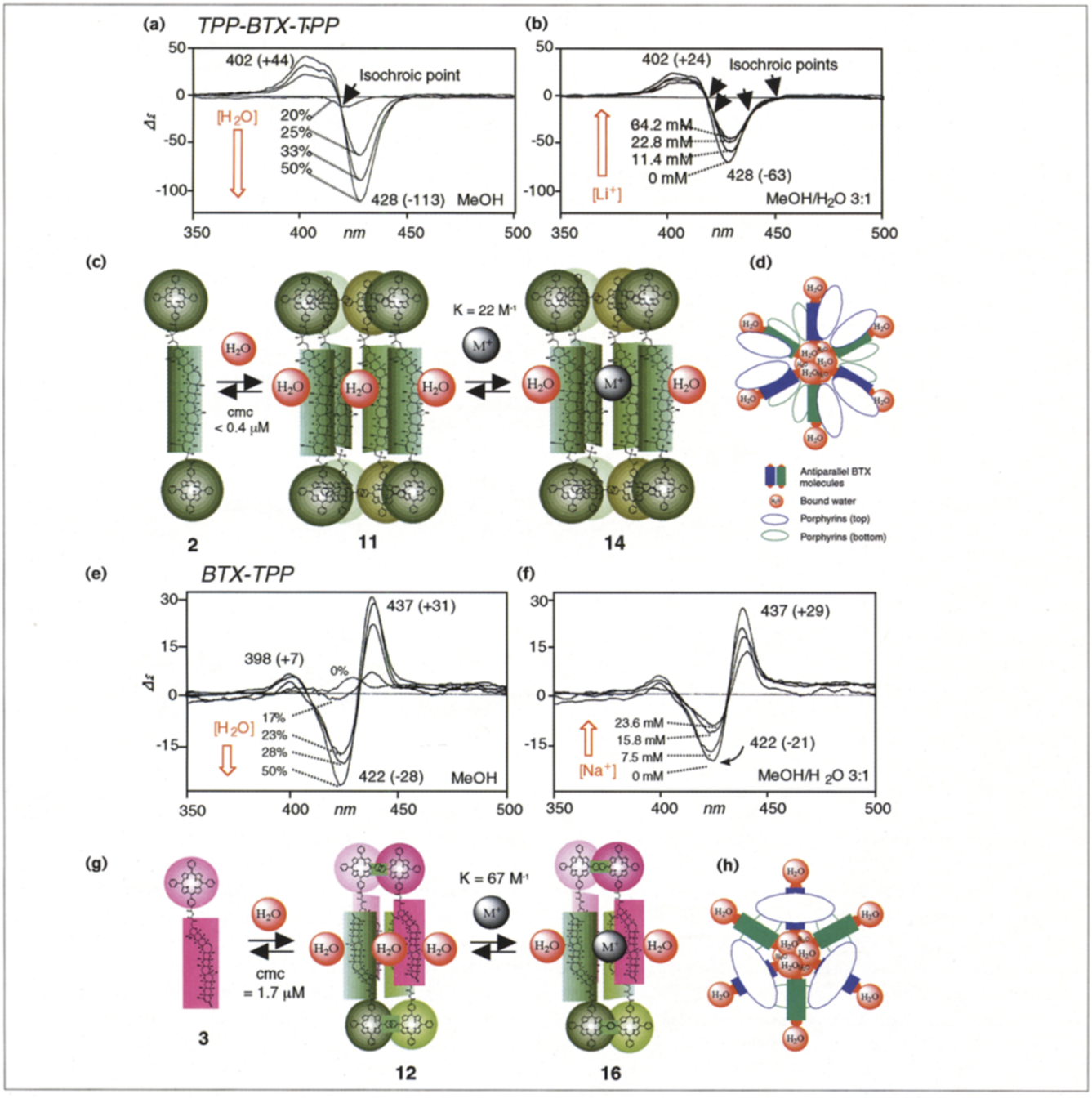

Self-assemblies and ionophoric properties of porphyrin-BTX conjugates in polar solvents. CD spectra resulting from **(a)** titration of a methanolic solution of TPP-BTX-TPP (**2**) with water and **(b)** titration of a solution of self-assembly **11** with 500 mM LiCl; titration with 500 mM NaCl, KCl and CsCl gave the same result within experimental error. **(c)** The proposed self-assembly and metal-binding process. **(d)** Top view of the proposed cylindrical supramolecule **11** containing an even number (here, six is chosen arbitrarily) of BTX molecules. Antiparallel molecules are shaded green and pink. In the side views **11** and **14**, the two BTXs in front (of an arbitrary total of six) are not shown for clarity. The antiparallel orientation of the BTX backbones is not depicted in the reaction scheme in (c), because the orientation of BTX backbones carrying labels at both ends (**2** and **4**) is not experimentally detectable in superstructures such as **11** and **14**. Antiparallel orientations in the bisporphyrin assembly are depicted in (d). CD spectra of **(e)** the titration of a methanolic solution of BTX-TPP (**3**) with water and **(f)** the titration of a solution of self-assembly **12** with 500 mM NaCl show that BTX-TPP does self-assemble, although at a higher cmc than that of TPP-BTX-TPP and that the self-assembly **12** binds to metal ions with a K value of 67 M^{-1}; titration with 500 mM LiCl, KCl, and CsCl gave the same result within experimental error. **(g)** Model of self-assembly and metal binding of mono-chromophoric BTX **3**. **(h)** Top view of the proposed cylindrical supramolecule **12** (see (d)). Antiparallel molecules are shaded green and pink. Green square in **12** and **16** indicates a hydrophobic phenyl interaction. $M^+ = Li^+$, Na^+, K^+ or Cs^+.

cyclic superstructure can be hydrogen-bonded to water, with no hydrophobic BTX backbone exposed to the polar medium; this would yield a channel consisting of a radial BTX superstructure filled with a highly organized water tube and π,π-stacked terminal porphyrin chromophores (**11**, Fig. 2c; also see below).

The CD of the BTX monoporphyrin assembly **12** has a maximal A of +59 (Fig. 2d). The maximal A of bisporphyrin assembly **11**, at –157 (Fig. 2a), is of opposite sign with a reduced amplitude per chromophoric group. This results from a different spatial arrangement of the reporter porphyrin groups. Since the distances between the BTX skeletons can be assumed to be similar in mono- and bischromophoric assemblies, the observed differences in the CD of **11** and **12** can be rationalized by antiparallel orientations of the BTX backbone in **11** and **12**. The relative orientations of the BTX termini is, however, only distinguishable experimentally in superstructures of mono-porphyrin **3** and not in those of bisprophyrins **2** or **4**. (We have thus depicted an antiparallel orientation of the BTX backbones only in the reaction sequence **3**→**12**→**16** (Fig. 2g) and not in **2**→**11**→**14** (Fig. 2c)). But as discussed above there is strong evidence that the BTX backbones in all the BTX superstructures have the same, antiparallel orientation, as indicated in Fig. 2d and h. In **12**, this antiparallel orientation gives rise to 1,3-stacking of chromophores attached to every other BTX molecule (a hypothetical possibility is depicted in Fig. 2h). The chromophores attached to all BTXs in **11** must necessarily be π,π-stacked (as shown in Fig. 2d), but π,π-stacking is absent in **12** (Fig. 2h). The presence of hydrophobic interactions between the pendant phenyl substituents, as depicted in **12**, instead gives rise to the observed difference in the organized porphyrin coupling mode.

The fact that the porphyrin interactions in **12** are less significant than those in **11** explains the difference in cmc between these two self-assemblies (1.7 μM for **12** as opposed to < 0.4 μM for **11**). Because of the weak mutual porphyrin interactions in **12**, the cmc of BTX-B (**1**) must be ≥ 1.7 μM in a 3:1-mixture of methanol and water. As the level of self-organization increases with increasing proportions of water in the solvent it follows that the cmc of BTX-B in pure water is likely to be << 1.7 μM, increasing the likelihood that BTX-B self-organization is biologically significant. (Higher order BTX polymers, such as ribbons, instead of self-assemblies **11** and **12**, could also form, and might be responsible for the weak blue-shifted Cotton effects [18], such as the peak at 398 nm in Fig. 2e. These points await further investigation).

Ionophoric properties of self-assembled brevetoxin conjugates

Titration of the self-assembly **11** in MeOH/water 3:1 with the cations Li^+, Na^+, K^+ and Cs^+ resulted in a decrease of CD amplitudes (Fig. 2b). Unlike the one-step self-assembly of **2** to form **11**, cation complexation of **11** to form **14** is a multistep reaction, as shown by the presence of at least two isochroic points (Fig. 2b). The overall cation-binding constant estimated from the change in CD amplitude [19] is 22 M^{-1}, which was the same for all investigated cations within experimental error. The monochromophoric self-assembly **12**, examined in the same way, revealed a three-fold higher, non-selective cation affinity (Fig. 2f). Since binding constants of self-assemblies are unknown in the literature, we must compare these values with those for cation complexes of monomeric BTX (see below).

Cations can bind either to the porphyrin moieties or to the polyether moieties of BTX porphyrin conjugates. Cation complexation to porphyrins seems to be negligible under the conditions of CD measurements, however, because the binding constant is smaller for the bis-chromophoric BTX self assembly **11** to form **14** (Fig. 2c, K = 22 M^{-1}) than for the porphyrin 'deficient' monochromophoric BTX self assembly **12** to form **16** (K = 67 M^{-1}). Furthermore, no CD change is observed upon cation addition to transmembrane bisporphyrin BTX self-assembly **15** (Fig. 4), in which only the porphyrins are exposed to the medium.

Upon cation complexation of **11** and **12**, the signs and shapes of the CD curves do not change but their amplitudes are diminished (Fig. 2b,f). This suggests that although the overall structures of **11** and **12** are conserved in complexes **14** and **16**, the interchromophoric distances (and thus the distances between BTX moieties in the complexes) are larger. In the cyclic superstructures **11** and **12** the oxygens of the BTX backbone form 'crown ether-like' rings. In the absence of cations, these rings are presumably filled with solvent. The water molecules that form hydrogen bonds to the BTX skeletons in **11** and **12** are replaced by cations in complexes **14** and **16**. To gain the required space for this complexation process, the attracting forces between the porphyrin chromophores must be overcome. This explains why the binding constant for bisporphyrin **11**, which has strong porphyrin interactions, is smaller than that for monoporphyrin **12**, which has weaker porphyrin interactions. It follows that the cation binding constant of self-assembled BTX-B should be >67 M^{-1} in MeOH/water 3:1.

Ionophoric properties of non-assembled brevetoxin conjugates

The hydrophilic TPyP-BTX-TPyP (**4**) does not form self-assembly **13** (Fig. 3a) in water at pH 4 in the conditions under which the CD measurements are taken, because of the charge repulsion of pyridinium cations. The non-conservative Cotton effect of A = –21 (Fig. 3b), which is concentration independent, is thus due to an intramolecular long-range coupling, occurring over a distance of up to 50 Å because of the intense electronic absorption of the porphyrin chromophore [11,12]. Cation binding of monomeric TPyP-BTX-TPyP (**4**) to Li^+, Na^+, K^+ and Cs^+

Figure 3

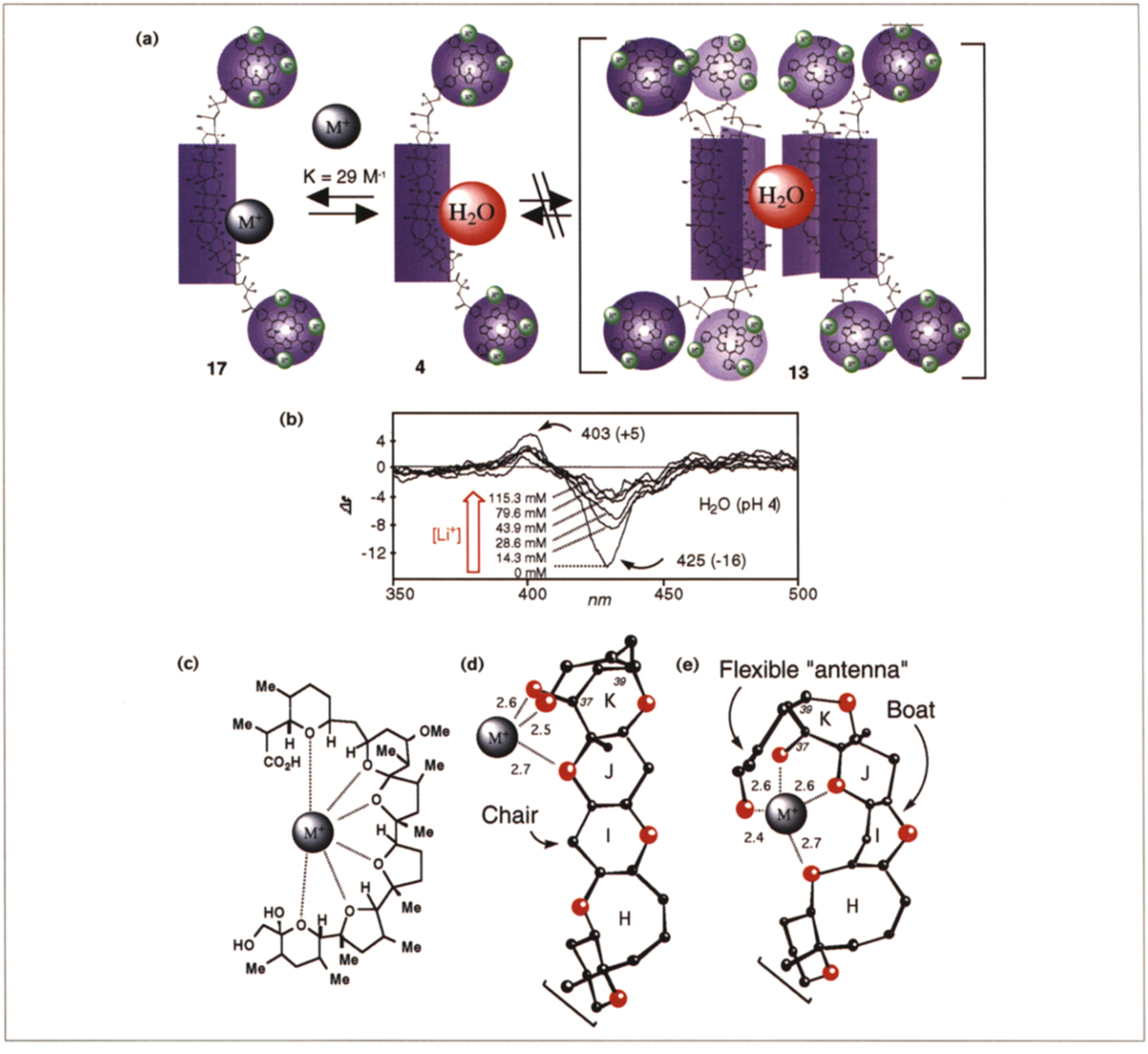

Cation binding by brevetoxin derivatives. **(a)** Cation-binding properties of TPyP-BTX-TPyP (**4**) in water, pH 4. This molecule binds non-specifically to cations, with a complex formation constant (K) of 29 M^{-1}. It does not form self-assembly **13** because of the charge repulsion of the pyridinium cations. **(b)** CD measurements of **4** in the presence of various concentrations of Li^+; titration with 500 mM NaCl, KCl and CsCl gave the same result within experimental error. **(c)** The binding characteristics of the antibiotic potassium carrier nigericin are similar to those determined here for **4** [22]; the cation complex of nigericin is shown. **(d)** Proposed cation complex of BTX-B calculated by MacroModel V4.5 [23] with the I-ring in chair configuration. $M^+ = Li^+$, Na^+, K^+, or Cs^+. **(e)** Alternative binding conformation in which ring I is boat-shaped, providing a possible intermediate stage in ion transport across the membrane.

was explored by titration of cations into an aqueous solution at pH 4. Cation addition was accompanied by a decrease in CD amplitude (Fig. 3b). The resulting overall complex formation constant is 29 M^{-1} and is non-specific for the measured cations within experimental error. The changes in CD are accounted for by conformational changes in the BTX skeleton, induced by formation of the cation complex **17** (again, cations would not bind to the triscationic porphyrins).

Ionophores in methanol and other organic solvents generally give rise to high complex formation constants, whereas in aqueous solutions the constants tend to be much lower [20] and are comparable to that observed for

BTX (K = 29 M^{-1}). For example, the potassium-selective ionophore nigericin (Fig. 3c) binds cations in aqueous solution in the same range as that of brevetoxin, with a K_K of 96 M^{-1} and a K_{Na} of 22 M^{-1} [21].

Where is the cation-binding site in isolated BTX-B molecules? Nigericin, a flexible polyether ionophore, creates a cavity around cations yielding a hexacoordinated complex structure [22] (Fig. 3c), but BTX-B is rigid. In the BTX molecule it is only at the ring K terminus that more than two oxygen ligands are available, namely the axial K-hydroxyl group (37-OH), the J-ring oxygen and the side chain aldehyde. MacroModel V4.5 [23] calculations show that the energy can be minimized around a hypothetical cation with distances of ~2.6 Å, an appropriate length for an O–Na bond (Fig. 3d). After binding the cation as in Figure 3d, the I-ring could adopt a boat conformation by virtue of the neighboring eight-membered H-ring, while the change in energy resulting from forming the unfavorable boat conformation (ΔE = +47 kJ mol^{-1} in the gas phase) could be offset by the binding energy of the additional H-ring oxygen ligand (Fig. 3e). The flexible aldehyde side chain could adjust the cation cavity size, allowing non-selective cation binding. This cation-binding model may account for the fact that the terminal substitution pattern at the axial 37-OH and axial 39 side-chain is conservative in brevetoxins and ciguatoxins. This region has unknown function, and its conservation is therefore surprising. We propose that in transmembrane BTX-B self-assemblies these terminal cation binding sites may act as ionophoric 'antennae' on the lipid surface, bringing the metal ions into the pore formed by the toxin molecules in the membrane.

Transmembrane self-assemblies of porphyrin-labeled BTX-B

Large unilamellar vesicles (LUVs) containing fresh egg yolk phosphatidyl choline (PC) and ~1.2 mol% porphyrin-labeled BTXs were prepared at pH 7.4 by Reynold's dialytic detergent removal technique [24]. Vesicles **15** containing TPP-BTX-TPP (Fig. 4a) give a strong negative split CD centered at 421 nm, A = −78 (Fig. 4b, solid line), which is similar to the negative-split CD of the TPP-BTX-TPP self-assembly **11** in polar solvents centered at 419 nm, A = −157 (Fig. 2a). Thus the bischromophoric TPP-BTX-TPP (**2**) forms self-assemblies (**15**, Fig. 4a) in lipid bilayers, the structure of which is similar to the self-assemblies formed in polar solvents. Treatment of the lipid emulsion of **15** with 100 mM HCl to lower the pH from 7.4 to 1.0 resulted in a bathochromic shift of the porphyrin Soret absorption from 418 nm to 436 nm (not shown). This showed that all chromophores in **15** become protonated and therefore must be in the aqueous phase or close to it. Thus the TPP-BTX-TPP self-assembly **15** has a transmembrane structure, and is not found in the middle of the lipid phase parallel to the vesicle surface.

The above experiment demonstrates that a transmembrane orientation of BTX self-assemblies is energetically favored over the hydrophobic TPP/lipid interaction. This transmembrane alignment can be accounted for by the fact that the rigid hydrophobic, cigar-shaped BTX skeleton has a length that corresponds to the thickness of bilayers. In the absence of vesicle rupture, the protonation accompanying the above-mentioned acidification of intravesicular porphyrins in the assembly **15** demonstrates that proton transport through the BTX channel occurs in the usual time-scale (seconds; [25] and references therein). The CD spectrum of TPP-BTX-TPP (**2**) in PC LUVs, pH 1, **18**, is devoid of extremes; thus, the biscationic porphyrin moieties in **18** do not undergo coupling in any self-organized fashion due to charge repulsion (Fig. 4a).

The following trends are seen in the CD spectra of monochromophoric BTX-TPP (**3**) (Fig. 4c): in PC vesicles (forming the emulsion shown as **19**) the spectrum shows only a broad negative absorption around 421 nm at pH 7.4 (see also Fig. 4b); however, the protonated species **20**, unlike protonated **18**, yields a clear bisignate split CD, similar in sign and shape to the spectrum of monochromophoric self-assembly **12** except for the bathochromic shift in the absorption spectrum of **20** due to protonation (436 nm). Thus, the structure of membrane-bound monochromophoric BTX **3** can be represented by a cyclic ('radial') self-assembly **20** with antiparallel oriented BTX and additional hydrophobic phenyl/phenyl attraction in the aqueous phase. In contrast to the porphyrin π,π-stacking in **15**, which is inhibited by protonation of the crowded bisporphyrin **18** (Fig. 4a), the appearance of a bisignate CD in the less crowded monoporphyrin **20** at pH 1 shows that porphyrin/porphyrin couplings are self-organized even under acidic conditions because of the longer distances between the charged porphyrin cores. Thus, the peripheral phenyl/phenyl attraction energetically overrides the unfavorable charge repulsion of the porphyrin chromophores.

In monochromophoric BTX-TPP the porphyrins are randomly immersed in the lipid phase close to the chiral lipid surface (Fig. 4d, **19**), giving rise to an uncharacteristic broad negative CD spectrum (Fig. 4b, dotted line). A similar situation is found in the water-soluble bischromophoric TPyP-BTX-TPyP **21** (Fig. 4e), which shows only a weak positive CD (Fig. 4b, dashed line); this weak CD disappears when the assembly is protonated to form **22**. The pentacationic porphyrins in protonated TPyP-BTX-TPyP **22** are released from the membrane surface, but further ordered ππ-stacking is inhibited by charge repulsion, as in the case of **18**. Because of the lack of clear coupled CD in hydrophilic **21**/**22**, there is no direct evidence for transmembrane BTX aggregation. Aggregation can, however, be expected, since the water-soluble trisanion BTX-BF (**5**) does show transmembrane self-assembly, as observed by fluorescence spectroscopy [7].

Figure 4

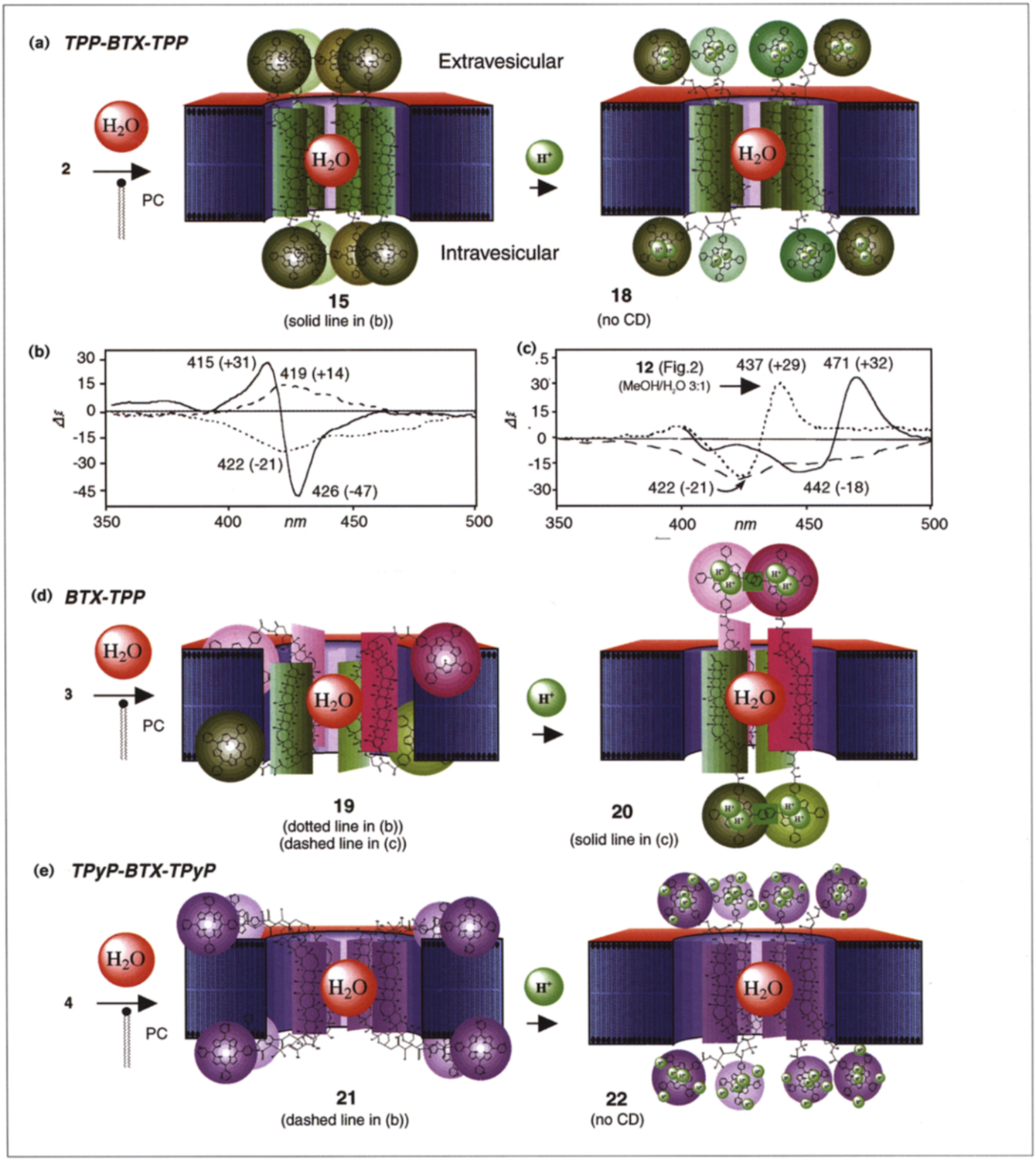

Self-assemblies of porphyrin BTX conjugates **2**–**4** in lipid bilayers. If possible, hydrophilic areas are given in red/violet, hydrophobic areas blue/green (see also Fig. 2). **(a)** Schematic drawing of the pores formed by TPP–BTX–TPP (**2**) in PC LUVs at pH 7.4 (left) and after lowering the pH to 1.0 with HCl (right). **(b)** CD curves of lipid-bound **2**–**4** at pH 7.4 (structures **15**, **19**, and **21**). **(c)** CD curves of monochromophoric BTX–TPP (**3**) in MeOH:water 3:1 (dotted, structure **12** in Fig. 2), in water/lipids pH 7.4 (dashed, **19**), and in water/lipids pH 1.0 (solid, **20**). **(d)** Schematic drawing of the pores formed by BTX–TPP (**3**) in PC LUVs at pH 7.4 (left) and after lowering the pH to 1.0 with HCl (right), and **(e)** schematic drawing of the pores formed by TPyP–BTX–TPyP (**4**) under the same conditions.

Structure–activity correlations

We have previously shown, using ^{23}Na NMR spectroscopic kinetic measurements, that vesicles containing 0.3 mol% BTX-B can conduct selective ion movement across lipid bilayers [7]. The same technique indicated that the fluorescence-labeled BTX-BF (**5**) [7] and CD-labeled BTX-TPP (**3**) also promote transmembrane ion movement, although at reduced rates. In the case of BTX-TPP (**3**), the brevetoxin concentration was increased four-fold (1.2 mol%) to reach a reasonable ratio of vesicle light scattering versus porphyrin absorption in the UV/VIS spectra. Control measurements ascertained that vesicle leakage caused by porphyrin-induced lipid oxidation was not detectable without irradiation [26]. Thus, we were able to confirm that porphyrin-labeled BTX (**3**) had ion-transporting properties in vesicles identical to those used for the CD measurements shown in Fig. 4. It is therefore possible to regard the superstructures for porphyrin-labeled BTXs shown in Figure 4a, d and e as representing the structures of native BTX-B pores.

The structure–activity correlations for BTX-TPP (**3**) and BTX-BF (**5**) clearly disagree. As discussed above, structural studies with porphyrin-labeled BTXs **2** and **3** imply that preformed BTX self-assemblies exist in polar solvents. On the other hand, the water-soluble pyrene derivative **5** self-assembles to form active superstructures only after incorporation into lipid bilayers, as detected by the blue-shift in the emission spectrum [7]. This difference leads to the conclusion that at least two divergent BTX pore-formation mechanisms must exist, depending on the cmc of the corresponding BTX derivative.

Cmc-controlled pore formation mechanisms

Pore formation kinetics was investigated according to a published protocol [25] with some modifications. Model vesicles (for example, egg PC LUVs), were prepared in the presence of the pH-sensitive fluorescent dye 5(6)-carboxyfluorescein (CF) at pH 7.4, in 90 mM NaCl and 10 mM LiCl buffer. After removal of the extravesicular CF by dialysis and/or size exclusion chromatography, the extravesicular pH was lowered to 6.4. Addition of the pore-forming molecule results in rapid proton influx reflected by the change in fluorescence intensity of the intravesicularly trapped CF (Fig. 5a). Because proton movement through a transmembrane pore is much faster than pore formation [25], the resulting kinetic curve reflects the rate-determining step(s) of pore formation.

Pore formation by BTX-B (**1**) and gramicidin, an antibiotic polypeptide with biologically significant ion-channel-forming properties [27], differ in rate but not in the apparent first-order kinetics of the reaction (Fig. 5b). The fact that the rate-limiting step for BTX-B is similar to that for gramicidin suggests that self-assembled BTX-B inserts into PC bilayers (Fig. 5c, 2→4), and shows that protons (i.e. protonated water ([28] and references therein)), can cross the BTX-pores. Pore formation by both gramicidin and BTX-B was measured over the concentration range 40 μM–500 nM. Preliminary results show that BTX pore formation is sensitive to several parameters other than concentration. In contrast to gramicidin, for example, pore formation by BTX-B is strongly increased upon application of additional ion gradients to the model system in Figure 5a, for instance by changing the 90 mM NaCl/10 mM LiCl medium to 10 mM NaCl/90 mM LiCl. This indicates that cations actively participate in BTX pore formation. Furthermore, treatment of vesicles with BTX in the presence of additional electric fields caused by an asymmetric cation distribution, for example a solution of 50 mM NaCl/50 mM LiCl or 99 mM NaCl/1 mM LiCl, containing vesicles with an internal solution of 90 mM NaCl/10 mM LiCl, strongly reduces BTX-B pore formation and proton influx (perhaps implying an overall BTX electric dipole moment which is perpendicular to its skeleton). This dependence of BTX pore formation on various parameters also shows that LUVs are rather primitive cell-membrane models, and that correlation of the observed trends with the nanomolar-level toxicity of BTX-B requires caution. Similar results were obtained with the closely related BTX-A (**23**) (Fig. 5d).

In contrast to the first-order kinetics of BTX-A, B and gramicidin, pore formation by the water-soluble BTX-BF (**5**) involves a more complex mechanism. A fast fluorescence increase is seen during the first 40 s, followed by a slow, almost linear, increase during the next 1000 s (Fig. 5b). Self-assembly of BTX-BF during pore formation was monitored *in situ* by measuring the previously reported 417 → 412 nm blue-shift in the cascade-blue emission maximum (excitation 360 nm) [7]. Since BTX-BF is monomeric in water (Fig. 5c, (i)), the BTX-BF monomers first enter the lipid bilayer (Fig. 5c, (iii)), then self-assemble within the lipid bilayer to form the active superstructure as characterized by fluorescence spectroscopy (Fig. 5c, (iv); [7]). Although we cannot rationalize the rate determining step(s) in the BTX-BF pathway at this stage, the kinetic measurements depicted in Fig. 5b unambiguously prove that there are at least two different cmc-controlled pore formation mechanisms for BTX-B and BTX-BF. In the case of BTX-BF, a 'flip-flop' of the negatively charged molecule leading to an active assembly with antiparallel molecules could be an additional rate-determining factor.

Discussion

Although the results of our studies on BTX porphyrin derivatives cannot be directly applied to BTX itself, several important conclusions can be derived regarding the tertiary structure of the ion-selective pore formed by BTX self-assembly. This pore has been shown to be sensitive to membrane composition (i.e. cholesterol content [7]) and

Figure 5

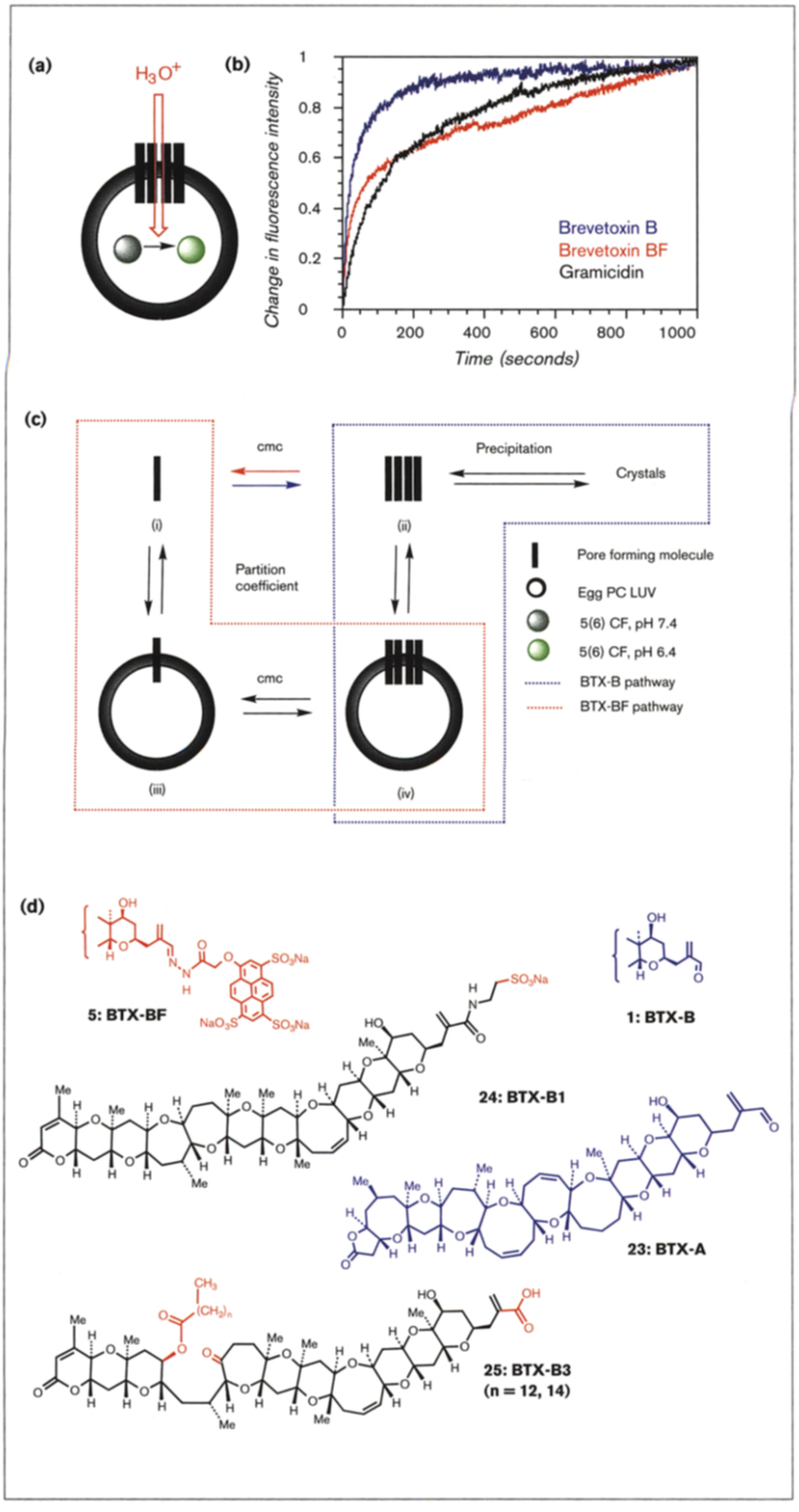

The pore formation activities of BTXs and gramicidin. **(a)** Schematic diagram of the system used here to measure pore formation kinetics [25]. A proton gradient is applied to a vesicle containing an entrapped pH-sensitive fluorescent probe. The rate-determining step(s) of pore formation is detected by monitoring changes in fluorescence emission at 520 nm as a function of time (excitation 470 nm). **(b)** Increase of fractional emission following the addition of 1 nmol pore-forming gramicidin or BTXs to 1 ml of polarized LUV solution (see Materials and methods). **(c)** Two different, cmc-controlled pore formation mechanisms: when cmc is low (BTX-B (**1**), BTX-A (**24**), blue), preformed pores (ii) enter the bilayer to establish the active transmembrane pore structure (iv). In the case of high cmc (BTX-BF (**5**), red), completely dissolved monomers (i) enter the bilayer (iii), and aggregate (iv). **(d)** The structures of several toxins are shown color-coded to their presumed mechanism of pore formation.

Figure 6

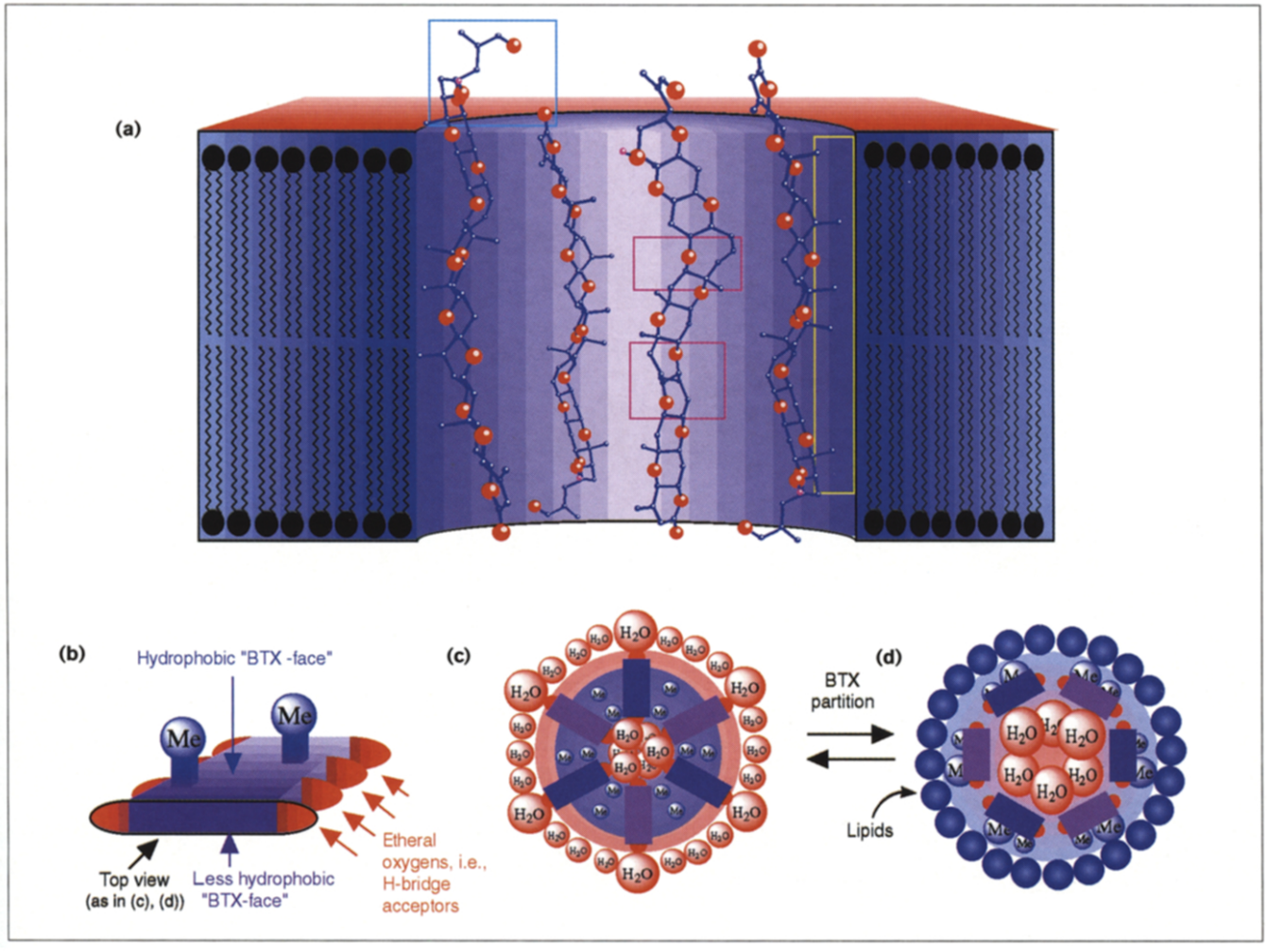

Model structures of BTX-B self-assemblies. Structural hydrophilicity is depicted as an increasing scale from blue to red. **(a)** Side view of a BTX-B transmembrane pore. An even number (here, six is chosen arbitrarily) of energy-minimized molecules is shown (MacroModel V4.5 [23]) BTX-B molecules are arranged cylindrically. The two BTX-B molecules in the front and all hydrogen atoms are not shown; carbon atoms (blue) are reduced in size and oxygen atoms (red) are enlarged for clarity. The modeled pores have the following characteristics: most of the methyl groups of the BTX-B backbone (yellow box) point toward the outside of the 'channel'; the K-terminal cation binding sites (cyan box) may act as ionophoric 'antennae' outside of the bilayer and assist in inserting ions into the pore; and the flexible D, E and H rings (magenta boxes) may serve as hinge regions assisting ion transport by undergoing conformational changes. **(b)** Schematic drawing of the BTX molecule, highlighting structural features that are important for pore formation. **(c)** Top view of an even number (six are shown) of self-assembled BTX-B molecules in polar solvents. The uncertain orientation of the interaction between the hydrophobic faces of the BTX-B skeleton is symbolized by loose methyl groups within the hydrophobic (dark violet) areas. **(d)** Top view of an even number (six) self-assembled BTX-B molecules in a lipid bilayer.

temperature [7], and here is shown to be sensitive to transmembrane electric fields, ion gradients, and the cmc of BTX-derivatives.

The model structure in Figure 6 summarizes our findings. Active, lipid-bound BTX-B can be considered to be a radial self-assembly with antiparallel BTX molecules aligned perpendicular to the membrane surface. In this model, an arbitrarily chosen even number of energy-minimized BTX-B molecules is arranged cylindrically in antiparallel orientations. The high number of oxygens in the pore cavity may be regarded as being analogous to tightly associated crown ethers, in which the contiguous crown ethers form the ion-selective pore [29]. Most of the methyl groups of the BTX-B backbone point toward the periphery of the pore (the hydrophobic 'BTX face', Fig. 6b), presumably interacting with the lipid molecules (Fig. 6d). This inherent amphiphilicity of the BTX skeleton suggests that the BTX self-assembly formed in lipid bilayers, where the hydrophobic 'BTX-face' interacts with the lipids (Fig. 6d) will be different from the superstructure formed in polar solvents, in which the hydrophobic

BTX-'faces' are buried within other BTX skeletons (Fig. 6c). Furthermore, we found that monomeric BTX-B binds non-specifically to cations in water ($K = 29\ M^{-1}$) and propose that the binding site is at the K-terminus. In transmembrane self-assemblies, the K-terminal cation binding sites may act as ionophoric 'antennae' outside the bilayer and assist in inserting ions into the pore (Figs. 6a, 3d,e). The hinge parts (the D, E and H-rings) could further assist in ion transport by conformational changes that allow 'breathing' in critical channel areas upon ion complexation.

The fact that comparable BTX self-assemblies are found in polar solutions might suggest that preformed BTX self-assemblies enter the lipid bilayer. But the water-soluble trianionic BTX-BF (**5**) and hexacationic TPyP-BTX-TPyP (**4**) are monomeric in water and aggregate, forming pores, only after incorporation into lipid bilayers (Fig. 5). Thus, aggregation in solution seems not to be important for channel activity in PC vesicles. As with amphotericin B, however, the cmc in solution alters the mechanism of pore formation in lipid bilayers, which may modulate the cell specificity of BTX pore formation [30].

The present study clarifies the interactions between brevetoxin molecules, cations and lipid bilayers. The fact that BTX and gramicidin have comparable activities (Fig. 5b), although their properties differ, indicates that BTX pore formation is likely to be significant under biologically relevant conditions. The relevance of the pore formation activity to BTX's ichthyotoxicity remains to be clarified, but it is possible that the two different, cmc-dependent BTX-pore forming mechanisms reported here could both be biologically important. The non-ichthyotoxic sulfonated brevetoxin B1 (**24**) was recently isolated from cockles. It was proposed that the K-terminal derivatization of this molecule is a self-defense mechanism (Fig. 5, [2]), preventing BTX-B from killing the cockle; the derivative is still toxic to mice and, presumably, to the mammalian predators of the cockle. The presence of the negatively charged sulfonate makes BTX-B1 (**24**) similar to the trisulfonate BTX-BF (**5**). The pore-forming mechanism of BTX-B1 might, therefore, be similar to that of BTX-BF. If so, the BTX-BF pathway would be expected to be non-toxic to fish (or cockles), but retain toxicity to mice. Compared to the extremely fast pore formation of BTX-B, that of BTX-BF follows a slower, higher order mechanism (Fig. 5b); it is possible that this may allow inhibition of the rate-determining step in fish but not in mice. If this is the case, the toxicity of BTX derivatives might be modulated and controlled by their cmc in water. We are now examining the toxicity of BTX-BF, and the correlation of cmc with the toxicity of BTX derivatives.

A different detoxification mechanism was proposed for the greenshell mussels *Perna canadiculus*, based on the isolation of BTX-B3 (**25**) [3]. It is thought that mussels that are being poisoned by exogenous BTX-B survive by oxidizing the terminal aldehyde and the D ring of the toxin to produce BTX-B3, which is not toxic to either fish or mice. This non-toxicity of **25** is consistent with the proposed pore-formation mechanism of self-assembled BTX-B: the cmc increases due to the terminal carboxylic acid, and the rigid 30 Å-long cigar-shaped skeleton of BTX-B, leading to favorable BTX-B/lipid interaction, is disrupted.

The high molecular weight maitotoxin [1] can be regarded as being a cross-linked BTX-B self-assembly; its high toxicity is the result of entropically favored cmc control in transmembrane self-assemblies. We are currently studying cross-linked BTX-B to find out whether it has similar characteristics.

Significance

The frequency and geographical distribution of massive fish kills (red tide) and human intoxication (shellfish poisoning) are rapidly increasing [1–3]. To prevent these disasters, and their socioeconomic consequences, we must start by understanding their scientific basis. Although a large number of polyether marine microbial toxins have been isolated, and their structures determined, the modes of action of these highly toxic compounds remain controversial. Brevetoxins, one of the first such toxins to be studied, have been shown to activate voltage-sensitive sodium channels [8]. We have recently found, however, that BTX-B can also directly induce selective cation transport through the membrane by forming transmembrane self-assemblies [7].

Here we have examined the supramolecular structures of the assemblies that brevetoxin forms, either on its own or in the presence of cations and lipids. We find that under biologically relevant conditions brevetoxin B self-assembles and can bind cations. The transmembrane BTX self-assemblies we describe here can mediate selective ion movement through membranes, and respond to temperature, lipid composition, electric fields, ion gradients, and the cmc of BTX-derivatives. The fact that BTX pores have similar activities to those formed by gramicidin underscores the potential biological significance of BTX pore formation in cell membranes. Although we do not yet know whether pore formation by BTX is important for its toxicity, we now have a clearer picture of the supramolecular chemistry and molecular structure of these toxins. This new understanding will inform future efforts to decipher the mode of action of polyether marine toxins.

Our previous [11–14] and present studies demonstrate the usefulness of porphyrin-reported exciton-coupled CD as a labeling technique to explore the molecular basis of activities of large structures such as the toxins studied here, and other biological molecules including proteins and nucleic acids.

Materials and methods

Preparation of compounds

Brevetoxin A (**23**) and B (**1**) were from an original stock [4], 'cascade blue' (**10**) was purchased from Molecular Probes Inc. Compounds **2–7** were prepared by chemical microscale synthesis as outlined in Figure 1 using standard laboratory procedures, purified by preparative thin layer chromatography or high-performance liquid chromatography (HPLC), and characterized by spectroscopic techniques. Materials, detailed procedure and spectroscopic data for all new compounds are available in the supplementary material. The preparation of **8** and **9** is also described in [14], and that of **5** in [7].

CD titrations

Most CD experiments are described in the text (Figs 2–4). Self-assemblies were prepared by titration of **2–4** in methanol with water (3.2 μM (**3**) or 1.6 μM (**2/4**)). CD spectra were normalized by correction of the dilution factor, absolute $\Delta\epsilon$-values were calculated on the basis of the extinction of monomeric **2–4** in methanol. Critical micelle concentrations (cmc's) were estimated by dilution of **3** (from 3.2 μM to 0.8 μM) and **2/4** (from 1.6 μM to 0.4 μM) in MeOH/water 3:1. CD spectra were normalized by correction of the dilution factor, absolute $\Delta\epsilon$ values were calculated on the basis of the concentration of monomeric **2–4**. Cation binding of self-assemblies was measured by titration of **2/3** in MeOH/water 3:1 with 500 mM LiCl, NaCl, KCl, CsCl solutions, respectively. Binding constants were calculated from at least two measurements following the method described by Blout and coworkers [19]. Binding constants of monomeric **4** were measured by titration of **4** in water (100 mM AcOH/$AcONH_4$, pH 4) with 500 mM LiCl, NaCl, KCl, CsCl solutions, respectively. CD spectra at pH 7.4 of lipid-bound BTX-porphyrins **15**, **20**, **21** were achieved by diluting the corresponding stock solutions with 100 mM LiCl, 10 mM Tris, pH 7.4 (see below). CD spectra at pH 1 of lipid-bound BTX-porphyrins **18**, **19**, **22** were achieved by diluting the corresponding stock solutions with 100 mM HCl, 10 mM Tris. Cation binding of lipid-bound BTX-porphyrins **15**, **20**, **21** were measured by titration with 500 mM LiCl, NaCl, KCl, CsCl solutions, respectively. All CD spectra were recorded on a JASCO J-720 spectropolarimeter driven by a JASCO DP700N data processor. Smoothing and other manipulations of spectra were carried out with software developed in house using a DFT (discrete Fourier transform) procedure for smoothing.

Vesicle preparation

As described in [7], large unilamellar vesicles were prepared following the dialytic detergent removal procedure of Reynolds and coworkers [24]. Fresh yolk egg PC (Sigma), octyl β-D-glucopyranoside (Sigma) and BTX derivatives in the molar ratio 1:15:0.003–0.012 (see text) were dissolved in 5 ml chloroform/methanol (HPLC grade) 2:1 and evaporated to a thin film. After complete removal of organic solvents and dissolution in 1 ml 100 mM LiCl, 10 mM Tris, pH 7.4, the resulting clear solution was dialyzed against 100 mM LiCl, 10 mM Tris, pH 7.4 (3 x 800 ml, 12 h, room temperature, dark). It was shown by ^{7}Li and ^{23}Na NMR spectroscopy that additional purification with Sephadex G-25 or Sepharose CL4B basically do not change the properties of the final solution. The lipid concentration was determined by phosphate digestion (see [7]) and correlated to the absorption (light scattering) at 300 nm, the BTX-porphyrin concentration was determined measuring the Soret absorption (412 nm) and/or by HPLC, the ratio of the intra- vs extravesicular volumes were determined with ^{7}Li NMR spectroscopy integrating the peaks for Li^{+}_{in} and Li^{+}_{out}.

Pore formation kinetics by fluorescence spectroscopy

Vesicle preparation was basically as described above (egg PC LUVs), but without any BTX derivatives. Dissolution and the initial dialysis (3 x 800 ml, 12 h, room temperature, dark) were performed with 20 μM 5(6) CF (Sigma), 90 mM NaCl, 10 mM LiCl 10 mM Tris, pH 7.4. The second dialysis (3 x 800 ml, 12 h, room temperature, dark) was done with 90 mM NaCl, 10 mM LiCl, 10 mM Tris, pH 7.4. Extravesicular 5(6) CF was completely removed after this dialysis as shown by Sepharose CL4B chromatography. In each kinetic measurement, 20 μl of the vesicular stock solution was added to 1 ml of pH 6.4 buffer (90 mM NaCl, 10 mM LiCl, 10 mM Tris), placed in a quartz cuvette and equilibrated for 20 min at 20 °C. This buffer was varied in the case when additional gradients (10 mM NaCl, 90 mM LiCl, 10 mM Tris, pH 6.4) or electric fields (50 mM NaCl, 50 mM LiCl, 10 mM Tris, pH 6.4; 99 mM NaCl, 1 mM LiCl, 10 mM Tris, pH 6.4) were applied. To the cuvette, 20 μl of gramicidin (in DMSO) or BTXs (in MeOH) were added with continuous monitoring of fluorescence emission at 520 nm in 0.5-s intervals (excitation 470 nm). The added amount of BTX and gramicidin ranged from 0.5 to 40 nmol, yielding final concentrations of 500 nM–40 μM. The resulting curves were normalized for comparison into the fractional change of fluorescence as described in [25]. Control experiments showed that addition of 20 μl MeOH results in no, and addition of 20 μl DMSO results in a very small, increase of emission at 520 nm. The turbidity of the vesicular emulsions did not decrease in the presence of BTXs or gramicidin, indicating the absence of detergent effects [25]. It was also confirmed by ^{23}Na NMR that the vesicles are not lysed under the experimental conditions; the intravesicular Na^{+} signal did not disappear within the experimental timescale.

Supplementary material available

The supplementary material contains materials, preparation procedures and spectroscopical data for all new compounds, ^{23}Na NMR spectroscopic activity plots for **1**, **3** and **5** including description of sample preparation and characterization, and cmc-related dilution plots for **11–13**.

Acknowledgements

We thank Dr J. Decatur for NMR assistance, and Dr N. Sakai and Professor P. Usherwood for discussions. This work was supported by NIH GM 34509, NIH AI 10187 and the Schweizerischer Nationalfonds (SM).

References

1. Yasumoto, T. & Murata, M. (1993). Marine toxins. *Chem. Rev.* **93**, 1897–1909.
2. Ishida, H., *et al.*, & Kosuge, T. (1995). BTX-B1, a new polyether marine toxin from the New Zealand shellfish, *Austrovenus stutchburyi*. *Tetrahedron Lett.* **36**, 725–728.
3. Morohashi, A., *et al.*, & Yasumoto, T. (1995). BTX-B3, a new brevetoxin analog isolated from greenshell mussel *Perna canaliculus* involved in neurotoxic shellfish poisoning in New Zealand. *Tetrahedron Lett.* **36**, 8995–8998.
4. Lin, Y.Y., *et al.*, & Nakanishi, K. (1981). Isolation and structure of BTX-B from the 'red tide' dinoflagellate *Ptychodiscus brevis* (*Gymnodinium breve*). *J. Am. Chem. Soc.* **103**, 6773–6775.
5. Shimizu, Y., Bando, H., Chou, H.-N., Van Dyne, G. & Clardy, J.C. (1986). Absolute configuration of brevetoxins. *J. Chem. Soc., Chem. Commun.* 1656–1658.
6. Nicolaou, K.C., *et al.*, & Unterstellar, E. (1995). Total synthesis of brevetoxin B. 2. Completion. *J. Am. Chem. Soc.* **117**, 1173–1174.
7. Matile, S. & Nakanishi, K. (1996). Selective cation movement across lipid bilayers containing brevetoxin B. *Angew. Chem. Int. Ed. Engl.* **35** 757–759.
8. Gawley, R.E., *et al.*, & Baden, D.G. (1995). The relationship of brevetoxin 'length' and A-ring functionality to binding and activity in neuronal sodium channels. *Chemistry & Biology* **2**, 533–541.
9. Czarnik, A.W. (1995). Desperately seeking sensors. *Chemistry & Biology* **2**, 423–428.
10. Hayes, J.J. (1995). Chemical probes of DNA structure in chromatin. *Chemistry & Biology* **2**, 127–135.
11. Matile, S., *et al.*, & Blagoev, B. (1995). Porphyrins: powerful chromophores for structural studies by exciton coupled circular dichroism. *J. Am. Chem. Soc.* **117**, 7021–7022.
12. Matile, S., Berova, N., Nakanishi, K., Fleischhauer, J. & Woody, R. (1996). Structural studies by exciton coupled circular dichroism over a large distance: porphyrin derivatives of steroids, dimeric steroids, and brevetoxin B. *J. Am. Chem. Soc.*, in press.
13. Matile, S., Berova, N. & Nakanishi, K. (1996). Intramolecular porphyrin π,π-stacking: assignment of absolute configuration of single chiral centers by exciton coupled circular dichroism. *Enantiomer*, in press.
14. Huang, D., Matile, S., Berova, N. & Nakanishi, K. (1996). Synthesis of philanthotoxin analogs with bulky heads. Self-assembly monitored by circular dichroism. *Heterocycles* **42**, 723–735.

15. Harada, N. & Nakanishi, K. (1983). *Circular dichroic spectroscopy – Exciton coupling in organic stereochemistry.* University Science Books, Mill Valley, CA.
16. Nakanishi, K. & Berova, N. (1994). The exciton chirality method. In *Circular dichroism – principles and applications.* (Nakanishi, K., Berova, N. & Woody, R.W., eds), VCH Publishers Inc., New York, NY.
17. Rein, K.S., Baden, D.G. & Gawley, R.E. (1994). Conformational analysis of the sodium channel modulator brevetoxin A, comparison with BTX-B conformations, and a hypothesis about the common pharmacophore of the 'site 5' toxins. *J. Org. Chem.* **59**, 2101–2106.
18. Fuhrhop, H.-J., Demoulin, C., Boettcher, C., Köning, J. & Siggel, U. (1992). Chiral micellar porphyrin fibers with 2-aminoglycosamide head groups. *J. Am. Chem. Soc.* **114**, 4159–4165.
19. Madison, V., Atreyi, M., Deber, C.M. & Blout, E.R. (1974). Cyclic peptides. IX. Conformations of a synthetic ion-binding cyclic peptide, *cyclo*-(Pro-Gly)$_3$, from circular dichroism and ^{1}H and ^{13}C nuclear magnetic resonance. *J. Am. Chem. Soc.* **96**, 6725–6734.
20. Izatt, R.M., Bradshaw, J.S., Nielsen, S.A., Lamb, J.D. & Christensen, J.J. (1985). Thermodynamic and kinetic data for cation-macrocycle interaction. *Chem. Rev.* **85**, 271–339.
21. Riddell, F.G., *et al.*, & Southon, T.E. (1988). The nigericin-mediated transport of sodium and potassium ions through phospholipid bilayers studied by ^{23}Na and ^{39}K NMR spectroscopy. *J. Am. Chem. Soc.* **110**, 734–738.
22. Hilgenfeld, R. & Saenger, W. (1982). Structural chemistry of natural and synthetic ionophores and their complexes with cations. *Top. Curr. Chem.* **101**, 3–82.
23. Mohamadi, F., *et al.*, & Still, W.C. (1990). MacroModel – an integrated software system for modeling organic and bioorganic molecules using molecular mechanics. *J. Comput. Chem.* **11**, 440–467.
24. Mimms, L.T., Zampighi, G., Nozaki, Y., Tanford, C. & Reynolds, J.A. (1981). Phospholipid vesicle formation and transmembrane protein incorporation using octyl glucoside. *Biochemistry* **20**, 833–840.
25. Ghadiri, M.R., Granja, J.R. & Buehler, L.K. (1994). Artificial transmembrane ion channels from self-assembling peptide nanotubes. *Nature* **369**, 301–304.
26. Berg, K. & Moan, J. (1994). Lysosomes as photochemical targets. *Int. J. Cancer* **59**, 814–822.
27. Woolley, G.A. & Wallace, B.A. (1992). Model ion channels: gramicidin and alamethicin. *J. Membrane Biol.* **129**, 109–136.
28. Feng, W.Y. & Lifshitz, C. (1995). Influence of multiple hydrogen bonding on reactivity: ion/molecule reactions of proton-bound 12-crown-4 ether and its mixed clusters with ammonia and methanol. *J. Am. Chem. Soc.* **117**, 11548–11554.
29. Murillo, O., Watanabe, S., Nakano, A. & Gokel, G. W. (1995). Synthetic models for transmembrane channels: structural variations that alter cation flux. *J. Am. Chem. Soc.* **117**, 7665–7679.
30. Yamashita, K., Janout, V., Bernard, E.M., Armstrong, D. & Regen, S.L. (1995). Micelle/monomer control over the membrane-disrupting properties of an amphiphilic antibiotic. *J. Am. Chem. Soc.* **117**, 6249–6253.